Two-Dimensional NMR Study on the Structures of Micelles of Sodium Taurocholate

Noriaki Funasaki,* Makoto Fukuba, Tomohiro Kitagawa, Masao Nomura, Seiji Ishikawa, Shun Hirota, and Saburo Neya†

Kyoto Pharmaceutical University, Misasagi, Yamashina-ku, Kyoto 607-8414, Japan

Received: July 23, 2003; In Final Form: October 1, 2003

The aggregation behavior of sodium taurocholate (TC) in deuterium oxide without salt was investigated by one- and two-dimensional NMR spectroscopy. Analysis of the concentration dependence of the chemical shift suggests that TC forms a dimer and a pentamer. The equilibrium constants of dimerization and pentamerization are close to those already determined by chromatography in the presence of 154 mM sodium chloride. The structure of the dimer is estimated from the NOESY and ROESY spectra of a 8 mM TC solution and molecular mechanics calculations. The inter-proton distances calculated from the molecular mechanics structure are consistent with the NOE and ROE intensities, whereas those calculated from the X-ray crystal structure (hydrogen-bonded structure) are inconsistent. The molecular mechanics structure is stabilized by hydrophobic interactions between the steroid nuclei and by reduced electrostatic repulsion between the sulfonate ions. The local structures of the pentamer are estimated on the basis of the ROESY spectrum of a 30 mM TC solution. The pentamer of TC is formed mainly by hydrophobic interactions. Thus, a novel NMR method in surfactant chemistry has provided the first step to resolve the 20-year debate about the structures of dimers and micelles of TC. This novel approach in surfactant chemistry will serve to estimate the structures of micelles of other natural and synthetic surfactants.

Introduction

The salts of bile acids are natural occurring, steroidal molecules. The micellization of bile salts plays a critical role in the digestion of lipids in animals. Many studies on this topic have been reported and reviewed from various viewpoints.[1−6] In comparison to synthetic surfactants, the bile salts have a different chemical structure. They have a few hydroxyl groups directed toward the concave side (often called the α plane in Figure 1) of the carbon framework and have the hydrophobic convex side (also called the β plane). This characteristic structure results in an aggregation pattern and a micellar structure much different from those of the synthetic surfactants.

Although the presence[1,2,4,7] or absence[3,8] of dimers and monodispersity[8] or polydispersity[1−4,9,10] in micelle size were matters of controversy, recent studies have indicated the presence of dimer and polydisperse micelles.[5,6,11−14] The exact mechanism of bile salt aggregation and the structure of the resulting aggregates in aqueous solution are still a matter of debate. According to the Small model,[1] the primary micelles of bile salt are formed by hydrophobic back-to-back interactions and larger secondary micelles are formed by mutual association of the primary micelles via intermolecular hydrogen bonding between the hydroxyl groups of the primary micelles. This model has been supported by a variety of experimental techniques, such as light scattering,[9] fluorescence probe method,[10,15] and gel filtration chromatography.[6,7,11,12] For instance, gel filtration chromatographic data allowed us to determine the dimerization constants (K_2) and critical micelle concentrations (cmc) of sodium taurocholate, taurodeoxycholate, taurochenodeoxycholate, and tauroursodeoxycholate in 154 mM sodium chloride solutions and to find quantitative relationships of K_2 and cmc with hydrophobic molecular surface areas.[7,12] The structure of larger micelles was also proposed on the basis of molecular mechanics calculations.[15] On the other hand, the face-to-face model of dimer via the hydrogen bonding between the hydroxyl groups of bile salt was proposed,[16] but this model was criticized.[17] A helical model for micelles of bile salts was proposed:[18,19] similar to reverse micelles, the helix is polar inside and nonpolar outside. A close network of hydrogen bonds, together with Coulombic interactions between the alkali metal cations and carboxylate (or sulfonate) groups of the bile salt and ion−dipole interactions between the alkali metal cations and water molecules have been suggested to be factors stabilizing the helix.[18] Surprisingly, the nonpolar faces (convex sides) of the bile salt molecules are oriented outward toward the bulk aqueous medium.[5]

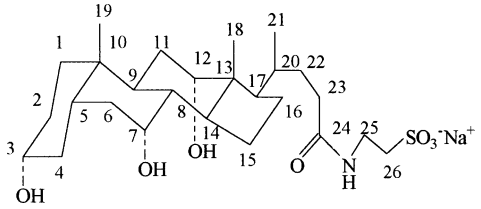

Figure 1. Chemical structure and labeling of carbons of TC.

Nuclear magnetic resonance spectroscopy (NMR) has been applied to estimate the micelle formation and micellar structure of bile salt.[19−26] Recently, the solution structures of biopolymers and inclusion complexes have been determined using the nuclear Overhauser effect (NOE) of NMR.[25−29] This powerful technique, however, has scarcely been employed to estimate the structures of micelles of surfactants including bile salt. The main purpose

* To whom correspondence should be addressed. Noriaki Funasaki, Ph.D., Kyoto Pharmaceutical University, Misasagi, Yamashina-ku, Kyoto 607-8414, Japan. Phone: +81-75-595-4663. Fax: +81-75-595-4762. E-mail: funasaki@mb.kyoto-phu.ac.jp.

† Present address: Graduate School of Pharmaceutical Sciences, Chiba University, Inage-Yayoi, Chiba 263-8522, Japan.

10.1021/jp030899h CCC: $27.50
Published on Web 12/11/2003

of the present work is to estimate the micellar structure of sodium taurocholate (TC) in deuterium oxide on the basis of two-dimensional NOE spectroscopy. It will be shown that the Small model is the best among the aggregation models for bile salts.

Experimental Section

Materials. Specimens of TC (Calbio) was treated with charcoal in methanol three times and recrystallized from methanol, as already reported.[7] The crystals were freeze-dried from water several times and dried at 383 K under reduced pressure. The purified samples of TC were both 99.0% pure or more, as estimated by high-performance liquid chromatography.[7] Methanol (Wako Pure Chemicals) and 99.9 at. % D deuterium oxide (Aldrich) were used as the internal standard and solvent, respectively.

NMR Measurements. All 500 MHz proton NMR spectra of deuterium oxide solutions were obtained with a JEOL Lambda 500 spectrometer at 298.2 ± 0.1 K. The proton chemical shift of TC, with reference to 0.1 mmol dm^{-3} (mM) internal methanol at 3.343 ppm,[29] was determined as a function of TC concentration (up to 20 mM).

Two-dimensional phase-sensitive rotating frame nuclear Overhauser effect spectroscopy (ROESY) for 1, 8, and 30 mM solutions were performed at 500 MHz with the JEOL standard pulse sequences; data consisted of 8 transients collected over 2048 complex points. A mixing time of 250 ms, a repetition delay of 1.2 s, and a 90° pulse width of 11.0 μs were used. The ROESY data set was processed by applying a Gaussian function in both dimensions and zero-filling to 2048 × 2048 real data points prior to Fourier transformation. Small cross-peaks, close to noise, were neglected. The NOESY spectrum for a solution containing 8 mM TC was also recorded at a mixing time of 150 ms with the JEOL standard pulse sequences. The ROE and NOE intensities were calculated with our own software. Two-dimensional CH COSY spectroscopy (CH COSY) for a 30 mM TC solution was performed at 500 MHz with the JEOL standard pulse sequences to establish assignments of protons and carbons of TC.

Molecular Modeling. The crystal structure of TC was used as a rigid body to model the structure of the dimer of TC.[19] The starting structure of the dimer was constructed on the basis of NMR data with our own molecular modeling software. The geometry of the dimer was optimized by molecular mechanics calculations in the presence of water on a Silicon Graphics Octane workstation. The Accelrys Insight II/Discover CVFF force field was used for energy minimization. Energy minimization was performed using the conjugate gradients method to a derivative of 0.001 kcal mol^{-1} with the Insight II′ default values (van der Waals' cut off distance = 0.95 nm and electrostatic cut off distance = 0.95 nm).[30]

Results

Chemical Shifts and Self-Association Equilibrium of TC. The assignments of carbons and protons of TC in NMR spectra were carried out on the basis of a CH COSY spectrum and the literature data.[20−26] Because the H12 signal around 4.1 ppm was apart from other signals and exhibited a larger change than other protons, its chemical shift, δ, could be determined accurately. The chemical shift of this proton is shown as a function of TC concentration, C, in Figure 2. The plots of δ vs C and vs $1/C$ yielded critical micelle concentration (cmc) values of 6.5 and 8.3 mM (literature values of 4.5 to 12 mM), respectively.[2,31] This large gap between these two cmc values determined on the basis of the same chemical shift data suggests that TC self-associates stepwise and noncritically, as already reported for TC in 150 mM sodium chloride solutions.[7,12,32]

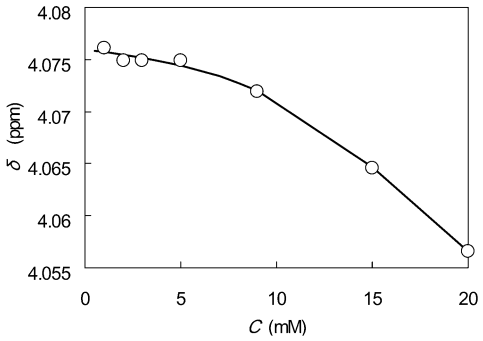

Figure 2. Concentration dependence of chemical shifts of proton H12 of TC: observed (○) and simulated (—) values on the basis of the dimerization-pentamerization model with equilibrium constants and chemical shifts given in Table 1.

TABLE 1: Equilibrium Constants and Chemical Shift Variations for Dimerization and Pentamerization of TC

K_2 (mM^{-1})	K_5 (mM^{-4})	δ_1 (ppm)	δ_2 (ppm)	δ_5 (ppm)
0.0062	7.85×10^{-7}	4.076	4.050	3.957
0.00611[a]	6.16×10^{-7}[a]			

[a] Value determined in 154 mM sodium chloride solution by gel filtration chromatography.[7]

The equilibrium constant of i-mer (TC_i) formation from i monomers is defined as

$$K_i = [TC_i]/C_1^{\,i} \tag{1}$$

where C_1 and $[TC_i]$ denote the molarities of monomer and i-mer of TC. For such a self-associating system the chemical shift is generally written as

$$\delta = \sum_{i=1}^{\infty} i[TC_i]\delta_i/C = \sum_{i=1}^{\infty} \Sigma i K_i C_1^{\,i}\delta_i/C \tag{2}$$

where δ_i is the chemical shift of i-mer. It is hard to estimate the values of K_i and δ_i for all species. On the basis of our chromatographic study on TC,[7] we presumed that TC forms dimer and m-mer alone. This approximation simplifies eq 2 to

$$\delta = (C_1\delta_1 + 2K_2 C_1^{\,2}\delta_2 + mK_m C_1^{\,m}\delta_m)/C \tag{3}$$

The best fitting of the parameters in eq 3 to the observed chemical shifts, shown by the solid line in Figure 2, yielded values of $m = 5$, three chemical shifts, and two equilibrium constants given in Table 1.

The equilibrium constants of self-association of TC in a 154 mM sodium chloride solution were determined by gel filtration chromatography (GFC).[7] The dimerization and pentamerization constants by NMR agreed well with those obtained by GFC, as shown in Table 1. In the 154 mM sodium chloride solution, TC forms hexamer and larger micelles, because electrostatic repulsion on the micellar surface is decreased by the presence of sodium chloride.

NOESY and ROESY Spectra and Structures of Monomer and Dimer. At 1 mM, TC does not form any aggregates. Interproton cross-peaks in NOESY and ROE spectra (data not shown) of 1 mM TC solution, therefore, will be ascribed to the proximity between the protons in a TC monomer. The volume (NOE and ROE intensity) of the cross-peak was determined by

TABLE 2: ROE/*N* and NOE/*N* Values for a 1 mM TC Solution and the Inter-Proton Distances for the X-ray Crystal Structure of TC.[19]

pair	ROE/*N*	NOE/*N*	d_{eff} (nm)
1α-1*β*	0.00	66.5	0.178
1α-19	0.77	1.4	0.282
2α-9α	0.00	38.5	0.205
3*β*-5*β*	0.00	3.4	0.272
4α-5*β*	0.00	14.4	0.301
5*β*-19	2.96	4.1	0.277
6α-6*β*	0.00	184.5	0.178
6α-7*β*	0.00	3.1	0.256
6*β*-7*β*	0.00	15.8	0.237
6*β*-8*β*	0.00	11.6	0.271
6*β*-19	9.44	5.2	0.249
7*β*-8*β*	0.00	26.3	0.231
7*β*-14α	3.85	1.0	0.300
7*β*-15α	0.21	0.0	0.255
8*β*-18	20.34	16.6	0.270
8*β*-19	19.20	13.2	0.248
11α-12*β*	0.00	12.0	0.247
11*β*-12*β*	0.00	14.3	0.243
11*β*-18	7.53	20.1	0.228
11*β*-19	1.93	1.6	0.255
12*β*-18	0.96	1.8	0.280
12*β*-21	46.53	6.6	0.224
14α-15α	0.00	8.0	0.237
15α-15*β*	0.00	101.5	0.178
15α-18	2.46	6.1	0.410
16α-17α	0.00	17.6	0.242
18−20	2.69	5.1	0.245
18−21	0.75	1.8	0.331
20−21	0.00	6.7	0.255

integration. Because the NOE and ROE intensities of the cross-peak are proportional to the number *N* of equivalent protons, NOE/*N* and ROE/*N* are correlated with the interproton distance. These ROE and NOE intensities are given in Table 2.

When internal rotations are slower than the overall tumbling, we can write the NOE or ROE intensity as[27,28]

$$\mathrm{NOE}/N = k d_{\mathrm{eff}}^{-6} \tag{4}$$

Here the effective distance, d_{eff}, is defined as[27,28]

$$(d_{\mathrm{eff}})^{-6} = (1/N) \sum_{i,j} d_{ij}^{-6} \tag{5}$$

In eq 4 and 5, *N* stands for the product of the numbers of equivalent protons in the groups corresponding to protons *i* and *j*. The d_{eff} value was calculated on the basis of the crystal structure of TC.[19] For protons H5*β* and H21, d_{eff} is 0.469 nm and *N* is 3. The distance between the protons that exhibited a cross-peak was lower than 0.41 nm (for protons 15α and 18). The largest cross-peak was observed for protons 6α and 6*β* (d_{eff} = 0.18 nm). The NOE/*N* values roughly obeyed eq 4. In the ROESY spectrum of 1 mM TC, the number of cross-peaks was smaller than that in the NOESY spectrum, because cross-peaks between protons spin−spin coupling with each other became smaller or disappeared in the ROESY spectrum.[27,28]

All data given in Table 2 are plotted in Figure 3 according to eq 4. The solid lines are drawn using eq 4 with the best fit values of $k = 0.003886$ and 0.003526 nm^6 for ROE/*N* and NOE/*N*, respectively. Good correlations indicate that the solution structure of TC monomer is close to the X-ray crystal structure.[19]

In the ROESY and NOESY spectra of a 8 mM TC solution, additional cross-peaks were observed. For instance, additional cross-peaks for three pairs of protons (H5*β*-H21, H7*β*-H18, and H8*β*-H21) are observed in the ROESY spectrum (Figure 4). The intensities of these peaks are given in Table 3. Because C_1

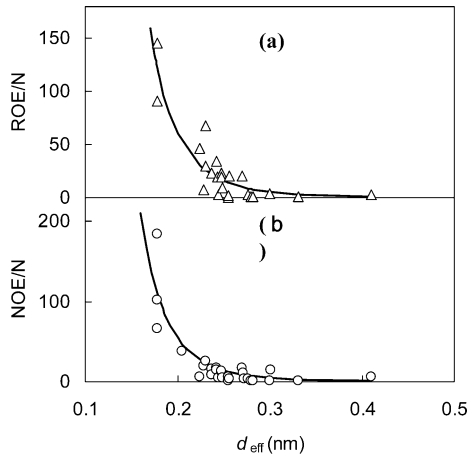

Figure 3. Correlation of (a) the observed ROE/*N* values (circles) and (b) the observed NOE/*N* values (triangles) with the effective distances calculated from the X-ray crystal structure of TC.[19] The ROE and NOE intensities are observed for 1 mM TC. The theoretical lines are calculated from eq 4.

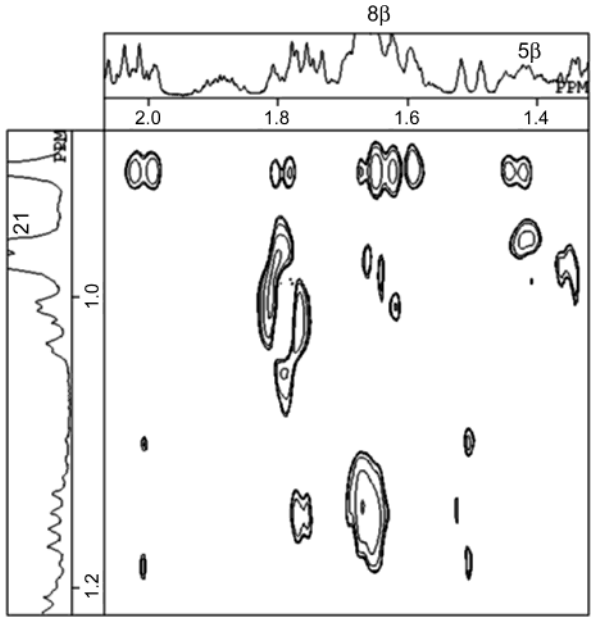

Figure 4. Contour plot of the NOESY spectrum of a 8 mM TC solution.

= 7.26 mM and $[TC_2]$ = 0.33 mM at 8 mM TC, as calculated using the dimerization and pentamerization constants given in Table 1, these additional peaks are ascribed to dimerization. The NOE/*N* and ROE/*N* values observed of a 8 mM TC solution are given in Table 3. From this table, the pairs given in Table 2 are removed, because we are concerned with the cross-peaks due to dimerization.

The dimeric structure of TC in crystals has been observed.[19] Using this dimer structure (Figure 5b), we calculated the effective distance between two intermolecular protons. As shown in triangles of Figure 6, the effective distances are too large for NOE cross-peaks to be observed usually.[28,33] We constructed a starting structure of the TC dimer consistent with the observed NOE and ROE data and optimized by molecular mechanics calculations. This optimized structure, shown in Figure 5a, allows us to calculate the effective distance. As shown in the circles of Figure 6, the correlation of the NOE and ROE intensities with the effective distance is good for the molecular mechanics structure. Cross-peaks in NOE and ROE spectra appear, when the inter-proton distance is usually below 0.4 nm

TABLE 3: ROE/*N* and NOE/*N* Values for 8 mM and 30 mM TC Solutions and the Corresponding Fragments Defined in Figure 7

pair[a]	8 mM NOE/*N*	ROE/*N*	30 mM ROE/*N*	fragments
1α−16β	0.0	0.0	75	ABF, PBF
1α−21	0.0	0.0	79	ABB, ABF
1β−4α	0.0	0.0	36	PBF
3β−8β	0.0	0.0	80	ABB, PBB
3β−9α	0.0	0.0	77	ABF, PBF
3β−21	0.0	0.0	102	ABB
4β−18	0.0	0.0	49	ABB
5β−18	0.0	0.0	409	ABB, PBB
5β−21	5.7	12.8	300	ABB
6β−12β	0.0	0.0	8	ABB, PBB
6β−16β	11.6	0.0	0	ABB, PBB
7β−9α	0.0	0.0	87	ABF, PBF
7β−15β	0.0	0.0	414	ABB, PBB
7β−16β	0.0	0.0	32	ABB, PBB
7β−18	2.3	7.4	26	ABB, PBB
7β−19	0.0	0.0	25	ABB, PBB
7β−21	0.0	0.0	2	ABB, PBB
8β−21	14.8	39.8	34	ABB, PBB, PBF
9α−12β	0.0	0.0	70	ABF, PBF
9α −18	0.0	0.0	24	ABF, PBF
12β−14α	0.0	0.0	15	ABF, PBF
12β−15α	0.0	0.0	1	ABF
16α−21	0.0	0.0	19	PBF
18−19	0.0	0.0	35	ABB, PBB

[a] All pairs given in Table 2 are omitted from this table, because they are close to each other in a TC molecule.

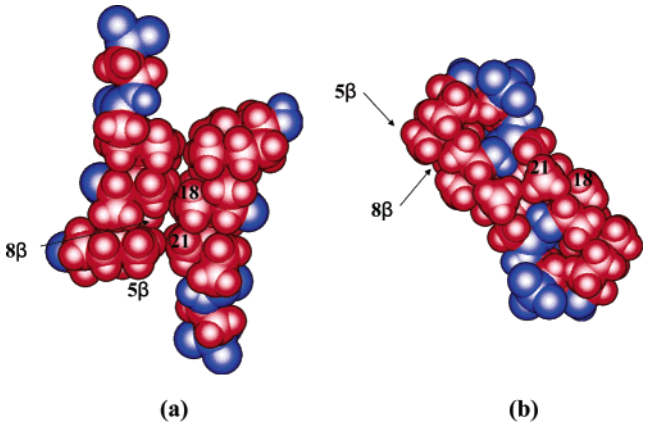

Figure 5. (a) Molecular-mechanics and (b) X-ray crystal structures of the TC dimer.

and sometimes below 0.6 nm. The effective distances between protons exhibiting cross-peaks for the crystal structure are larger than 0.84 nm, whereas those for the molecular mechanics structure are smaller than 0.65 nm. Therefore, our molecular mechanics structure (Figure 5a) of the TC dimer is much better than the crystal structure (Figure 5b).

Structure of Micelles. Many cross-peaks were observed in the ROESY spectrum of a 30 mM TC solution (data not shown). Because $C_1 = 18.15$ mM, $[TC_2] = 2.05$ mM, and $[TC_5] = 1.55$ mM at 30 mM, as calculated using the dimerization and pentamerization constants given in Table 1, these additional peaks are ascribed to micelles and dimers. The ROE intensities of these peaks are given in Table 3. Most of these peaks are not observed at 8 mM TC and will be ascribed to the formation of micelles. From this table all of the pairs given for the TC monomer in Table 2 are removed, because we are concerned with the cross-peaks due to micellization.

Although NMR will be a powerful method for detecting local structures of a micelle, it is not always suitable to estimate the

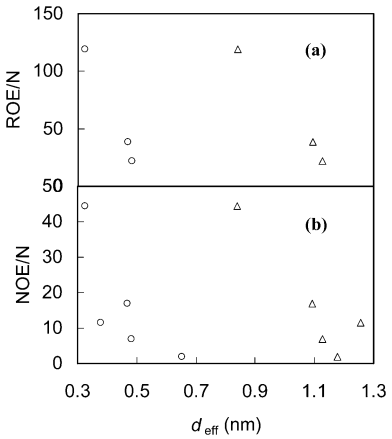

Figure 6. Correlation of (a) the observed ROE/*N* and (b) the observed NOE/*N* values with the effective distances calculated for two structures of the TC dimer: the molecular mechanics (circles) and X-ray crystal (triangles) structures shown in Figure 5.

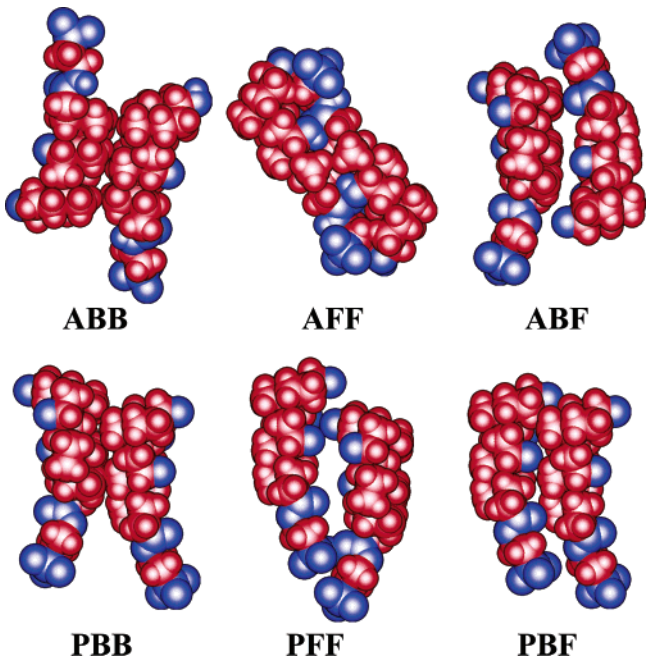

Figure 7. Six possible dimeric fragments of TC micelles: ABB, antiparallel back-to-back; AFF, antiparallel face-to-face; ABF, antiparallel back-to-face; PBB, parallel back-to-back; PFF, parallel face-to-face; PBF, parallel back-to-face. These dimeric fragments should be regarded as having some flexibility. Structure ABB is identical to the molecular mechanics structure of TC dimer (Figure 5a), and the structure AFF is the crystal structure of the TC dimer (Figure 5b) taken from ref 19.

whole structure of the micelle. We considered six basic dimeric fragments of TC micelles, which are observed in the models for the micelles already proposed in the literature.[1,15,16,20] Structure ABB (antiparallel back-to-back) is identical to that shown in Figure 5a. This structure is stabilized both by enhanced hydrophobic interactions between the hydrophobic steroid nuclei and a reduced repulsion between the sulfonate ions. The electrostatic repulsion between the sulfonate ions is also weak in structures AFF (antiparallel face-to-face) and ABF (antiparallel back-to-face), whereas it is strong in structures PBB (parallel back-to-back), PFF (parallel face-to-face), and PBF (parallel back-to-face). Structure AFF is observed in the X-ray crystal structure, shown in Figure 5b. Structure PBB is stabilized by enhanced hydrophobic interactions between the hydrophobic steroid nuclei. Structures AFF and PFF will be stabilized by

hydrogen bonding between hydroxyl groups. Structures ABF and PBF will be unstable because the hydrophobic back is in contact with the hydrophilic face in these structures. We regarded each of these six structures of dimeric fragments as the representative of more disordered structures.

The β protons and trimethyl protons 18, 19, and 21 of TC are at the backside, whereas the α protons are at the face side (Figure 1). Although trimethyl protons H21 are at the backside in the crystal structure, they can be at the face side by internal rotation of the C17−C20 bond. By assuming that the ROE cross-peak appears for a pair of protons being closer than 0.6 nm, we sought structures that are consistent with the pairs given in Table 3. These structures are given in Table 3. Even if structures AFF and PFF are present, they will be not detected by the ROESY and NOESY spectra. Therefore, the data in Table 3 do not indicate the absence of these structures.

The ROE intensity becomes larger with decreasing distance and is proportional to the concentration of species. Fragment ABB is the major component, whereas fragments ABF, PBB, and PBF are minor components.

Discussion

The chemical shift of proton H12 was used to estimate the self-association pattern of TC. The cmc values of 6.5 and 8.3 mM are in the range of the literature values of 4.5−12 mM.[31] The dimer and pentamer alone were regarded as aggregates, and equilibrium constants of dimerization and pentamerization are close to those determined by gel filtration chromatography (Table 1). Chromatography and mass spectroscopy indicate the presence of the TC dimer.[7,13] Chromatography is a very good method for detecting the dimer.[7] The TC micellar aggregation number of 5 is reasonable in comparison with the literature values in water.[1,2] This finding does not deny that other aggregates are present.[34] When we take into consideration more aggregate species, we need a relationship between the equilibrium constant and the aggregation number as well as a relationship between the chemical shift variation and the aggregation number.[7,34] The chemical shift (δ_i) of *i*-mer in eq 2 will change monotonically with an increase in the aggregation number *i*. However, it is difficult to predict this change theoretically. The chemical shifts of protons in the interior of the dimer and micelles will exhibit larger variations than those in the exterior. Very recently, we found a quantitative relationship between the chemical shift variation and the structure for the complexes of α-cyclodextrin with alkyltrimethylammonium bromides.[35] However, such a relationship for micellization of bile salts is not available. Thus, the chemical shift is not a very good quantity for investigating the self-association pattern. Therefore, we did not determine the concentration dependence of the chemical shifts of other protons of TC and did not apply other self-association models.

As shown in Table 1, the dimerization and pentamerization constants of TC in deuterium oxide determined by NMR are close to those obtained by gel filtration chromatography in a 154 mM sodium chloride solution.[7] Sodium chloride decreases the electrostatic repulsion among TC molecules at the micellar surface and salts out TC from the intermicellar solution. Furthermore, it was recently found that the binding constant of cyclodextrin with a guest molecule in deuterium oxide (D_2O) is larger than in hydrogen oxide (H_2O) by 5−20%. Therefore, the dimerization and pentamerization constants of TC in D_2O may be larger than those in H_2O.[36] The cancellation of these effects may result in close dimerization and pentamerization constants obtained by the two methods.

The solution structure of the TC monomer is close to the crystal structure (Figure 3). This finding indicates that the steroid nucleus of the TC monomer is rigid. From the ROE and NOE intensities for a 8 mM TC solution, we estimated the solution structure of TC dimer (Figure 5a). However, ROE and NOE cross-peaks were observed between protons being more distant than 0.6 nm (Figure 6). The structure of the dimer shown in Figure 5a should be regarded as the time-average structure. Therefore, two TC molecules can rapidly change the relative position with time, so that pairs of protons can approach more closely with each other than shown in Figure 5a. Therefore, Figure 5a shows the time-average structure of TC dimers.

According to Small, primary small micelles of bile salt are formed by hydrophobic interactions and that secondary larger micelles are formed by hydrogen bonds of the primary micelles.[1] Li and McGown energy-optimized the structures of micelles of bile salt by molecular mechanics calculations and obtained micellar structures similar to the Small model.[15] Without salt, TC will form the primary small micelles alone. These micelles are composed of fragments ABB and PBB. The present NMR data are consistent with these micelles. However, fragments ABF and PBF are present as minor components.

In crystals, TC forms dimers and helices composed of multiples of trimers.[19] These dimer and trimer are stabilized by polar interactions among the headgroups. It was suggested that these structures of dimers and trimers (reverse micelles) exist in water.[18] However, the observed small degrees of counterion binding are also inconsistent with the reverse-micelle model.[11,12] The Small model was supported by proton NMR data,[20] molecular mechanical calculations,[15] and chromatography.[4,6,7,11,12] The reciprocal of cmc and the dimerization constant increase proportionally with an increase in hydrophobic molecular area of bile salt.[12] These data are consistent with the present NMR data. Recently, we have found that the solution structure of the propanol-α-cyclodextrin complex is much different from the crystal structure.[29] This difference was explained in terms of intermolecular interactions: hydrophobic and hydrophilic interactions play a predominant role in the stabilization of the three-dimensional structure in aqueous solution, although electrostatic and hydrogen-bonding interactions will be major forces in crystals. The concept of molecular recognition by hydrophobic and hydrophilic interactions has been proposed.[29]

In conclusion, the concentration dependence of the chemical shift of TC is explicable in terms of dimerization and pentamerization. The structure of the TC dimer is consistent with back-to-back hydrophobic aggregation model, whereas it is inconsistent with the face-to-face hydrogen-bonding model. The structures of TC micelles are explicable by the Small hydrophobic aggregation model, though some disordered structures must be taken into consideration. Thus, the 20-year debate about the structures of dimers and small micelles of TC below 30 mM in the absence of salt has been resolved, although those of large micelles of dihydroxy bile salt still remain unsolved. The present important conclusion was derived by quantitative analysis of two-dimensional NOESY and ROESY spectra. This novel approach in surfactant chemistry will serve to estimate the structures of micelles of other natural and synthetic surfactants in the presence and absence of salt.

Acknowledgment. The present work was supported by a Grant-in-Aid for the Frontier Research Program from the Ministry of Education, Science, Sports, and Culture of Japan, which is gratefully acknowledged.

References and Notes

(1) Small, D. M. The Physical Chemistry of Cholanic Acids. In *Chemistry*; *The Bile Acids*; Nair, P. P., Kritchevsky, D., Eds.; Plenum Press: New York, 1971; Vol. 1, Chapter 8.

(2) Carey, M. C. Physical-Chemical Properties of Bile Acids and Salts. In *Sterols and Bile Acids*; Danielsson, H., Sjovall, J., Eds.; Elsevier: Amsterdam, The Netherlands, 1985; Chapter 8.

(3) Kratohvil, J. P. *Adv. Colloid Interface Sci*. **1986**, *26*, 131.

(4) Funasaki, N. *Adv. Colloid Interface Sci*. **1993**, *43*, 87.

(5) Hinze, W. L.; Hu, W.; Quina, F. H.; Mohammadzai, I. U. Bile Acid/Salt Surfactant Systems. In *Bile Acid/Salt Surfactant Systems*; Hinze, W. L., Ed.; *Organized Assemblies in Chemical Analysis*; JAI Press: Stamford, CT, 2000; Vol. 2, Chapter 1.

(6) Funasaki, N. Study of Bile Salt Association by Gel Filtration Chromatography. In *Bile Acid/Salt Surfactant Systems*; Hinze, W. L., Ed.; *Organized Assemblies in Chemical Analysis*; JAI Press: Stamford, CT, 2000; Vol. 2, Chapter 2.

(7) Funasaki, N.; Ueshiba, R.; Hada, S.; Neya, S. *J. Phys. Chem*. **1994**, *98*, 11541 and references therein.

(8) Liu, C. L. *J. Phys. Chem. B* **1997**, *101*, 7055.

(9) Mazer, N. A.; Carey, M. C.; Kwasnick, R. F.; Benedek, G. B. *Biochemistry* **1979**, *18*, 3064.

(10) Li, G.; McGown, L. B. *J. Phys. Chem*. **1993**, *97*, 6745.

(11) Funasaki, N.; Hada, S.; Neya, S. *J. Phys. Chem. B* **1999**, *103*, 169 and references therein.

(12) Funasaki, N.; Nomura, M.; Ishikawa, S.; Neya, S. *J. Phys. Chem. B* **2000**, *104*, 7745 and references therein.

(13) Rodríguez, M. A.; Yost, R. A. *Rapid Commun. Mass Spectrom*. **2000**, *14*, 1398.

(14) Matsuoka, K.; Moroi, Y. *Biochim. Biophys. Acta* **2002**, *1580*, 189.

(15) Li, G.; McGown, L. B. *J. Phys. Chem*. **1994**, *98*, 13711.

(16) Oakenfull, D. G.; Fisher, L. R. *J. Phys. Chem*. **1980**, *84*, 936.

(17) Zana, R. *J. Phys. Chem*. **1978**, *82*, 2440.

(18) Bonincontro, A.; D'Archivio, A. A.; Galantini, L.; Giglio, E.; Punzo, F. *J. Phys. Chem. B* **1999**, *103*, 4986.

(19) Campanelli, A. R.; Candeloro De Sanctis, S.; D'Archivio, A. A.; Giglio, E.; Scaramuzza, L. *J. Inclusion Phenomena* **1991**, *11*, 247.

(20) Small, D. M.; Penkett, S. A.; Chapman, D. *Biochim. Biophys. Acta* **1969**, *176*, 178.

(21) Murata, Y.; Sugihara, G.; Fukushima, K.; Tanaka, M.; Matsushita, K. *J. Phys. Chem.* **1982**, *86*, 4690.

(22) Barnes, S.; Geckle, J. M. *Lipid Res*. **1982**, *23*, 161.

(23) Campredon, M.; Quiroa, V.; Thevand, A.; Iiouche, A.; Pouzard, G. *Magn. Reson. Chem.* **1986**, *24*, 624.

(24) Stevens, R. D.; Ribeiro, A. A.; Lack, L.; Killenberg, P. G. *J. Lipid Res*. **1992**, *33*, 21.

(25) Liu, M.; Farrant, R. D.; Sweatman, B. C.; Nicholson, J. K. Lindon, J. C. *J. Magn. Reson. A* **1995**, *113*, 251.

(26) Leibfritz, D.; Roberts, J. D. *J. Am. Chem. Soc*. **1973**, *95*, 4996.

(27) Neuhaus, D.; Williamson, M. P. *The Nuclear Overhauser Effect in Structural and Conformational Analysis*, 2nd ed.; Wiley-VCH: New York, 2000; Chapters 5, 9, and 12.

(28) Croasmun, W. R.; Carlson, R. M. K. *Two-dimensional NMR Spectroscopy*, 2nd ed.; Wiley-VCH: New York, 1994.

(29) Funasaki, N.; Ishikawa, S.; Neya, S. *J. Phys. Chem. B* **2002**, *106*, 6431.

(30) *Insight II*, version 2000; Accelrys: San Diego, CA.

(31) Carey, M. C.; Small, D. M. *J. Colloid Interface Sci*. **1969**, *31*, 382.

(32) Kratohvil, J. P.; Hsu, W. P.; Jacobs, M. A.; Aminabhavi, T. M.; Mukunoki, Y. *Colloid Polym. Sci*. **1983**, *261*, 781.

(33) Schneider, H.-J.; Hacket, F.; Rüdiger, V.; Ikeda, H. *Chem. Rev*. **1998**, *98*, 1755.

(34) Funasaki, N.; Shim, H.-S.; Hada, S. *J. Phys. Chem*. **1992**, *96*, 1998. For a nonionic surfactant, it was difficult to distinguish between the stepwise aggregation model and the dimer plus single aggregate model on the basis of chromatographic data.

(35) Funasaki, N. Ishikawa, S.; Neya, S. *J. Phys. Chem. B* **2003**, *107*, 10094.

(36) Rekharsky, M. V.; Inoue, Y. *J. Am. Chem. Soc*. **2002**, *124*, 12361.